Final Draft
of the original manuscript:

Wahle, K.; Stanev, E.V.:

Consistency and complementarity of different coastal ocean observations: A neural network-based analysis for the German Bight

In: Geophysical Research Letters (2011) AGU

DOI: 10.1029/2011GL047070

Consistency and Complementarity of Different Coastal Ocean Observations. A Neural Network-based Analysis for the German Bight

K. Wahle,[1] E. V. Stanev,[1]

[1]Helmholtz-Zentrum Geesthacht,

Max-Planck-Str. 1, 21502 Geesthacht,

Germany.

Abstract

HF radar measurements in the German Bight and their consistency with other available observations were analyzed. First, an empirical orthogonal function (EOF) analysis of the radial component of the surface current measured by one radar was performed. Afterwards, Neural Networks (NNs) were trained to now- and forecast the first five EOFs from tide gauge measurements. The inverse problem, *i.e.* to forecast a sea level from these EOFs was also solved using NNs. For both problems, the influence of wind measurements on the nowcast/forecast accuracy was quantified. The forecast improves if HF radar data are used in combination with wind data. Analysis of the upscaling potential of HF radar measurements demonstrated that information from one radar station in the German Bight is representative of an area larger than the observational domain and could contribute to correcting information from biased observations or numerical models.

1. Introduction

High-Frequency (HF) radars measure the radial components of the surface current vector in the coastal ocean over space scales up to hundreds of kilometers, and on temporal scales starting from tens of minutes, thus providing a strong component for monitoring and prediction systems off the coastal ocean [*Emery et al.*, 2004; *Shay et al.*, 2007; *Barth et al.*, 2009]. For a large number of applications the consistency of HF radar data with other available observations needs to be quantified. This concern motivates the present research. In particular, a synergy is sought with data which are known to be of good quality (*e.g.* from tide gauges). Furthermore, use is made of as many as possible data sources (HF radar, tide gauges, wind observations and an ADCP), with a focus on short-term prediction capabilities based on observations, including skill estimates. Finally, the fundamental research question is addressed: can open shelf state estimates benefit from coastal ocean observations, or said with other words: do HF radar data enable upscaling in the sense of making reasonable predictions of the remote large-scale environment not sampled by HF radars?

2. Data and Methods

HF radar data from the Wellen Radar (WERA) system [*Gurgel et al.*, 1999] were used. One HF radar was installed on the island of Wangerooge (see Fig. 1a). The radar operated at a center frequency of 13 MHz. Data used in this study are the radial components of the surface current measured with a spatial resolution of 2×2 km taken almost continuously in January 2010 with a coherent integration time of approximately four minutes. The dynamics in the area covered by the radar are dominated by M2 tidal wave propagating from west to east along the southern coast of the German Bight, then turning to the north following the eastern coast.

Empirical orthogonal function (EOF) analysis is used to compress the radar dataset. Because the spatial coverage varied from measurement-to-measurement, a spatial and temporal subsample of the original dataset was needed, which did not contain gaps in space, allowing to perform EOF analysis. Here, the spatial resolution was reduced to 4×4 km by taking the averages of one to four points on the original grid. Only grid points with high data coverage were kept (this spatial subdomain containing 430 grid points is shown in Fig.1a). Observations which did not cover this subdomain were eliminated. After this processing, 3,426 of the original 9,258 measurements were left for the EOF analysis. In the following, the first five EOFs were used which altogether describe 92% of the variance. Horizontal patterns are not shown, because statistical characteristics of the radial velocity reflected not only physical processes, but also the specific observational setup. The projection of the data onto the dominant EOF-1 (describing 58% of the variance) presented as a function of time *modulo* M_2 duration (Fig1b) was instructive as a demonstration of the variability associated with the dominant M_2 tide. The beat frequency was due to the spring-neap-cycle.

Other observations used in this study were coastal sea level data from seven tide gauges (see planimetric symbols in Fig.1a for locations), wind data at 10m (u_{10}, v_{10}) from Heligoland, wind data at 33m (u_{33}, v_{33}) and current data at 2m from FINO-1 research platform. Figure1c shows the temporal variability of the sea level from the tide gauge in Büsum. Gauge data are available every 10 minutes; those taken at times of radar measurements used for the EOF analysis are marked. In Figure1d, the same representation was chosen for the hourly wind data from Heligoland. Variability found in the data, including several storm events was considered to be representative of different weather conditions in the area under study. At the FINO-1 platform, the mean current speed of 0.65m/s with a standard deviation of 0.25m/s was estimated from measurements with an ADCP. Overall, the meridional current component is weaker then the zonal one and more variable, the tidal oscillation in this direction being less pronounced.

The consistency of the HF radar data with the other observations will be analyzed using Neural Networks (NNs). NNs, as well as Self-Organizing Maps, are well applicable to identifying physical processes and dynamically distinctive spatial and temporal structures in HF radar data [*Liu et al.*, 2007]. For the training of the NNs, a pre-existing program [*Schiller*, 2000] was used. About 90% of the data was chosen randomly for the training of the NNs; the remaining part was kept as independent testing data (see Fig.1c,d).

3. State estimates in the HF radar area based on independent observations and Neural Networks

The first step was the reconstruction of the first five EOFs of the radar measurements from the data of the seven tide gauges. The sea level data from the tide gauges were used at the time of the radar measurement, plus those taken 1.5 and 3 hours earlier (NN1). This choice of input data was motivated by the size of the area, the typical current velocities, and the fact that the latter depend on the time derivative of the sea level. Alternatively, the same reconstruction using only the three gauges at Borkum, Büsum and Heligoland was carried out (NN2). Finally, a forecast of the five EOFs using only the seven gauges measured 1.5 and 3 hours before the radar observation (NN3) was performed. The NNs architectures giving the best performances are summarized in Table 1.

Fig.2 shows the reconstruction error defined as the root mean square (rms) difference between the reconstructed radar data and the original data. The radials reconstructed directly from the first five EOF modes can be considered as the "best possible performance" giving the smallest overall error of about 0.05m/s. This performance improves further with an increasing number of EOFs. For example, the improvement is quite noticeable, east and south of Heligoland Island, a region of complex hydrodynamics where the reconstruction using five EOFs gives errors up to 0.1m/s.

The reconstruction errors when applying NNs(1-3) to this testing dataset are overall below 0.1m/s Compared to the "best possible performance", the proposed methods show a similar spatial distribution of the errors but with higher absolute values. The nowcast using seven gauges (NN1) is slightly better than the one using only three (NN2). The forecast (NN3) performs almost as well as the nowcast, which is an important result.

To further improve forecasting skill, *i.e*, to approach the reconstruction error of the "best possible performance", hourly wind data (u_{10}, v_{10}) from Heligoland were used as an additional input to the NN. This choice was motivated by earlier research [*Barth et al.*, 2011] that demonstrated wind forcing for a numerical model can also benefit from the HF radar observations. A comparison of the performances of the forecasts without using wind data (NN3) and with using wind data (NN4) on the whole testing dataset was carried out, as well as on two subsamples with relatively high ($>$10m/s) and low ($<$1m/s) winds. The inclusion of the wind improved the forecast skill during the stormy period. Calm winds did not contribute to a noticeable improvement.

4. Predicting ocean state based upon HF radar observations

The inverse problem, *i.e.*, to forecast the ocean state which here is defined by sea level and ocean currents, outside the area covered by HF radar from the first five EOFs of the HF radar measurements, is considered in the following. The prediction of the sea level at the position of the tide gauge at Cuxhaven two hours ahead is first addressed. The problem may appear too "exotic" for practical applications; however, it has been chosen to illustrate the consistency between radials from only one HF radar station, which give incomplete information about currents and sea level from tide gauges, which is a signal that can be trusted. Furthermore, this mapping of one radial velocity component onto clear physical variables was aimed at removing uncertainties associated with specific instrumental designs.

Two NNs were trained. Input to both NNs are the five EOFs of radial velocity. For one of them wind data (u_{10}, v_{10}) from the island of Heligoland were also used. Each NN has one output; *i.e*, the sea level at Cuxhaven two hours ahead.

Scatterplots of the sea level at the tide gauge station as forecasted by the NNs versus the observed data (Fig.3a) illustrate the performance of the two networks. The inset displays the distribution of the differences between observation and forecast. The first two plots refer to the forecast without (NN5) and with (NN6) using the wind data, respectively. The forecast taking into consideration the wind performs considerably better. Its rms error is 8.4cm lower than in the case when wind data were not used. This result demonstrates that substantial complementarity could be expected if HF radar data would be used in combination with wind data when estimating sea level in the coastal ocean.

To check representativeness of analyses based on radial components of the surface current from one station only, the forecast skill when predicting current velocities perpendicular to the Wangerooge station radial direction with data from two radars instead of one was estimated. Although the improvement of about 0.2 could be considered in practical applications, it was relatively small, thus justifying the analysis presented here based on data from one station only.

Recent developments in oceanography have demonstrated that downscaling substantially improves the quality of state estimates in the coastal sea. The potential of upscaling, which is here understood as aggregation of the effects of small-scale coastal processes on the large-scale dynamics, is still not well understood. To analyze the upscaling potential of the HF radar data, a NN was trained to forecast currents outside the HF radar array coverage. Current data from the FINO-1 platform with ten minutes temporal resolution were used for training and testing the NN. Input to this NN7 consisted of the first five EOFs from the radial velocity and the wind measurement from the FINO-1 platform. Outputs were the two current components at FINO-1, two hours ahead. Applying NN7 to the testing data (left column in Fig.3b) demonstrated a very good skill. To simplify the interpretation of the NN results, current components from FINO-1 station were transformed into components parallel and perpendicular to the HF radar radial direction. The difference in rms error estimates for the two components is below 1cm/s. But the slope found with linear regression deviates more from unity for the perpendicular component.

To perform an evaluation of the quality of results, an alternative NN for forecasting the current components was constructed. Input to this NN8 consisted only of the tidal component of the currents at FINO-1 station and the wind data. Output was again the current (tidal and non-tidal) vector at FINO-1 station. The extraction of the tidal component was based on a tidal analysis of the observed data using the software package T-TIDE [*Pawlowicz et al.*, 2002]. Results of applying NN8 to the testing data (right column in Fig.3b) reveal a very reasonable skill, with the rms error being 5cm/s higher for the parallel component. Again, the slope of the regression line for the perpendicular component deviates more from unity. Presumably, the differences in forecasting the two current components for both, NN7 and NN8, originate from the dominant M2 being almost a zonal current (parallel component) at FINO-1, whereas the meridional current (perpendicular component) is mainly non-tidal.

The comparison between the corresponding panels of Fig.3b demonstrate that, although the HF radar observations did not reach the FINO-1 platform, the forecast based on coastal HF radar data outperformed the one from the simple partial tide synthesis model. This result indicates that forecasts based on HF radar data could be superior compared to the ones based on a modeling approach; in the present case, tidal analysis and the associated forecast played the role of one very simple and imperfect model.

5. Conclusions

The quality of forecasts for leading EOFs of HF radar-measured radial surface current velocities using Neural Networks and data from tide gauges and wind measurements was estimated as quite good, as compared to errors in observations and methods used. Solving the inverse problem, that is to forecast the sea level at a gauge station, was addressed in order to compare the performance of NNs to high-quality data from tide gauges. In either case, a forecast of 1.5 to 2 hours ahead appeared to have a good accuracy. Adding the wind data to the input information resulted in an improvement of sea level forecast at the location of the tide gauge, especially under stormy weather.

The consistency and complementarity between data of different sources was investigated in an experiment aiming at forecasting currents outside the domain of HF radar data. This experiment could only work provided good correlation existed between two independent velocity data sets, as was proven to be the case here. Furthermore, it demonstrated that information from radars in the German Bight could contribute to "repair" information from biased observations or models. Outputs from large scale numerical models could be considered as such biased information. The present research could motivate (1) future use of the presented techniques and (2) studies on upscaling of coastal observations, which could be considered as a contribution of coastal observatories to regional predictions in shelf seas.

Acknowledgments. We are grateful to J. Seeman, K.-W. Gurgel and F. Ziemer for making data from COSYNA observatory available and J. Schultz-Stellenfleth, C.N.K. Mooers and A. Barth for the motivating discussions and help in improving the paper.

References

Barth, A., A. Alvera-Azcárate, J.-M. Beckers, R. H. Weisberg, L. Vandenbulcke, F. Lenartz, and M. Rixen (2009), Dynamically constrained ensemble perturbations - application to tides on the West Florida Shelf, *Ocean Sci., 5,* 259-270.

Barth, A., A. Alvera-Azcárate, J.-M. Beckers, J. Staneva, E. V. Stanev, J. Schulz-Stelleneth (2011), Correcting surface winds by assimilating High-Frequency Radar surface currents in the German Bight, *Ocean Dynamics* DOI: 10.1007/s10236-010-0369-0.

Emery, B. M., L. Washburn, and J. A. Harlan (2004), Evaluating radial current measurements from CODAR high-frequency radars with moored current meters, *J. Atmos. Oceanic Technol., 21,* 1259-1271.

Gurgel, K.-W., G. Antonischki, H.-H. Essen, and T. Schlick (1999), Wellen Radar (WERA), a new ground-wave-based HF radar for ocean remote sensing, *Coastal Eng., 37,* 219-234.

Liu ,Y., R.H. Weisberg, and L.K. Shay (2007), Current patterns on the West Florida Shelf from joint Self-Organizing Map analyses of HF radar and ADCP data, *Journal of Atmospheric and Oceanic Technology, 24(4),* 702-712.

Pawlowicz R., R. Beardsley, and S. Lentz (2002), Classical tidal harmonic analysis including error estimates in MATLAB using T_TIDE, *Computers & Geosciences 28,* 929-937.

Schiller H. (2000), Feedforward–backpropagation neural net program ffbp1.0, *GKSS–report 2000/37,* ISSN 0344–9629.

Shay, L. K., J. Martinez-Pedraja, T. M. Cook, B. K. Haus, and R. H. Weisberg (2007), High frequency radar surface current mapping using WERA, *J. Atmos. Oceanogr. Tech. 24,* 484-503.

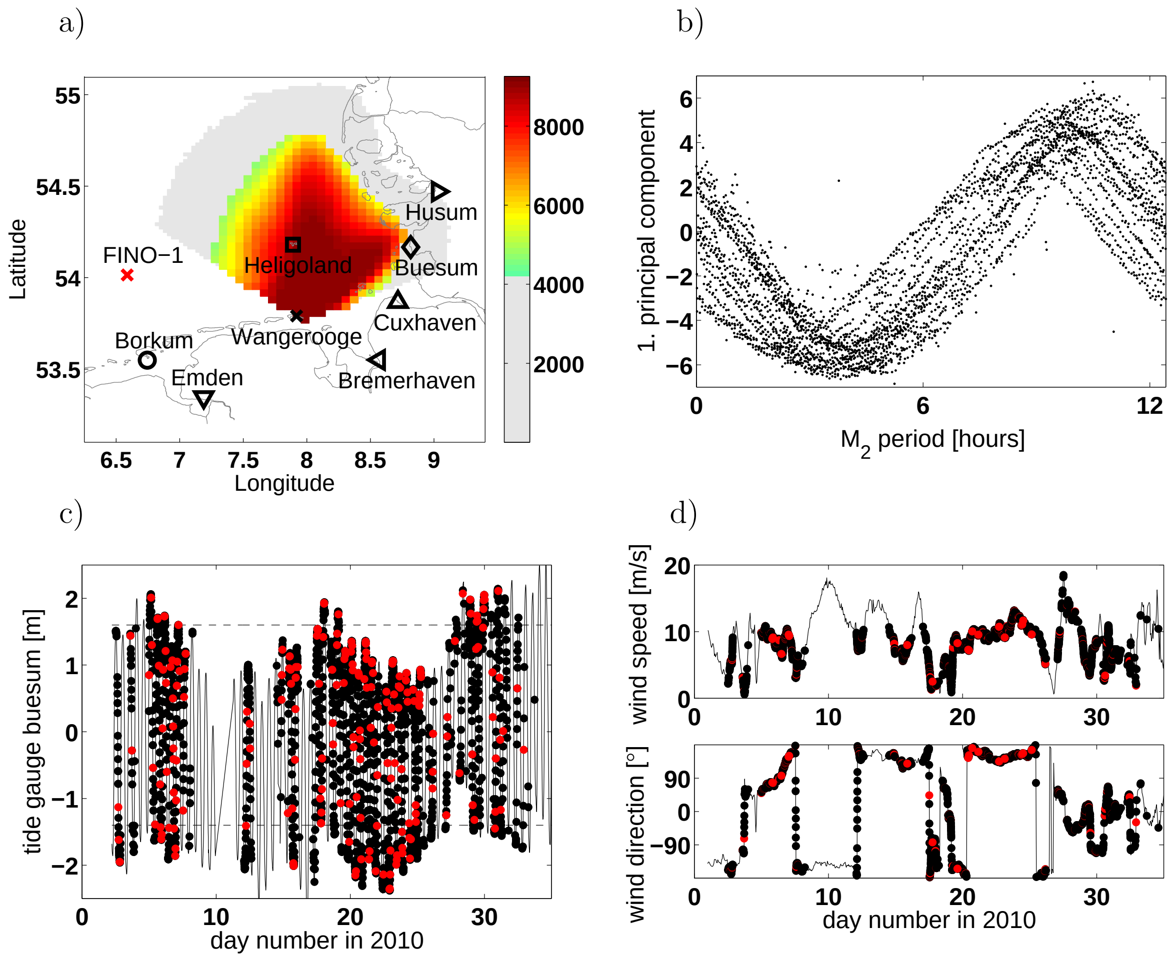

Figure 1. a) The number of available data in the German Bight provided by HF radar at Wangerooge in January 2010. Positions of stations mentioned in text are given by symbols.The grey area indicates the maximum spatial coverage of the radar system. b) Dominant PC as a function of time *modulo* M2 period. c) Sea level from the tide gauge at Büsum station as a function of time. Dashed lines indicate mean high (low) water. Black (red) dots indicate measurements used for training (testing) of Neural Networks. d) Graphical representation as in c) but for wind measurements on Heligoland.

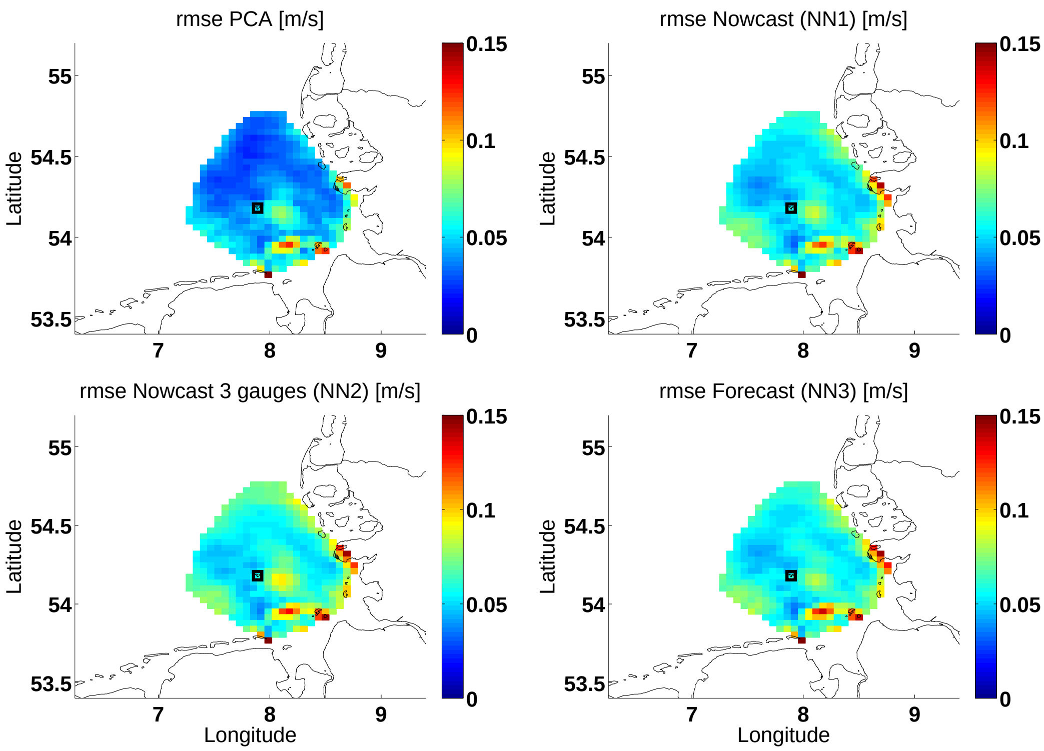

Figure 2. Spatial distribution of the root mean square error (m/s) of the reconstructed radar data from the original ones when applying different approaches to the test sample data. The top left figure refers to reconstruction with the original EOFs, and the remaining figures to reconstruction from EOFs calculated by NN(1-3) (see Table 1). The position of the Island of Heligoland (black square) is also given to localize areas of maximum errors.

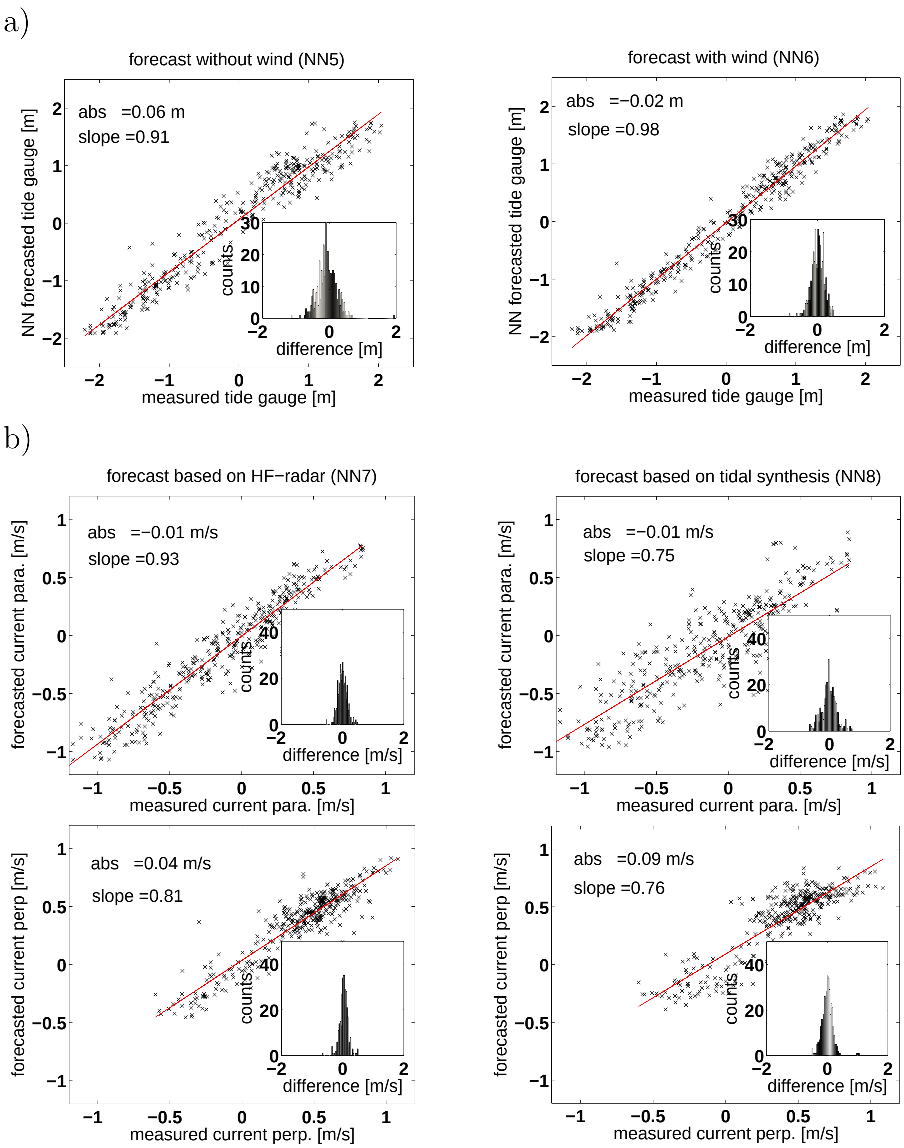

Figure 3. a) Performance of NN5 and NN6 (see Table 1) when forecasting the tide gauge signal at Cuxhaven. The sea level as forecasted by the NNs versus observations for all test data is shown. The red lines were calculated using linear regression. "Slope" gives the slope of the regression line, "abs" gives the axis intercept. The distribution of the differences between measured and forecasted sea levels is given in the insets. b) Graphical representation as in a) but for performances of NN7 and NN8 (see Table 1) which forecast the currents (here plotted as components parallel (top row) and perpendicular (bottom row) to the radial direction of the HF radar) at FINO-1 station.

name	input layer	hidden layer(s)	output layer
NN1	7 sea levels $t = 0, -1.5, -3$h	15x8	5 EOFs $t = 0$h
NN2	3 sea levels $t = 0, -1.5, -3$h	15x8	5 EOFs $t = 0$h
NN3	7 sea levels $t = 0, -1.5$h	20	5 EOFs $t = +1.5$h
NN4	7 sea levels $t = 0, -1.5$h, wind $t = -1.5$h, $[-6.5, -1.5$h$]$	20x8	5 EOFs $t = +1.5$h
NN5	5 EOFs $t = 0$h	15x10	sea level $t = +2$h
NN6	5 EOFs $t = 0$h, wind $t = 0$h, $[-5, 0$h$]$,	15x7x5	sea level $t = +2$h
NN7	5 EOFs $t = 0$h, wind $t = 0$h, $[-5, 0$h$]$,	20x10x6	FINO-1 current $t = +2$h
NN8	tidal current $t = 0$h, wind $t = 0$h, $[-5, 0$h$]$,	20x10x6	FINO-1 current $t = +2$h

Table 1. Architectures of the various Neural Networks discussed. For the wind input data, squared brackets indicate time intervals for averaging. The numbers in the third column give the number of neurons in each hidden layer: *e.g.*, NN1 has two hidden layers with 15 and 8 neurons, respectively.